Baseline Determination for Drive Cycle Performance Analysis of Permanent Magnet Synchronous Motors

Pawan Kumar Dhakal
Electric Drives and Machines Institute
Graz University of Technology
Graz, Austria
pawan.dhakal@tugraz.at

Kourosh Heidarikani
Electric Drives and Machines Institute
Graz University of Technology
Graz, Austria
k.heidarikani@tugraz.at

Roland Seebacher
Electric Drives and Machines Institute
Graz University of Technology
Graz, Austria
roland.seebacher@tugraz.at

Annette Muetze
Electric Drives and Machines Institute
Graz University of Technology
Graz, Austria
muetze@tugraz.at

***Abstract*—The popularity of Permanent Magnet Synchronous Motors (PMSMs) in electric vehicles (EVs) can be attributed to their impressive power and torque density, high-speed capabilities, and quick dynamic response. In contrast, Induction Motors (IMs) are known for their cost-effectiveness, robustness, ease of control, and superior performance at higher speeds. These motors also differ in terms of rotor losses, overload capacities, application, and industry standards. In the context of analyzing the overall performance of electric drives with these machines across various torque-speed operating points, significant computational effort and time are required. To address this, torque-speed performance maps, also known as efficiency maps, are commonly utilized. However, as these maps are primarily constructed for steady-state operation, their reliability in analyzing transient conditions remains uncertain. This paper presents a baseline for the assessment of the confidence in performance analysis using performance map-based approaches compared to time-stepping analysis of dynamic drive cycles. The evaluation is conducted using a laboratory-based PMSM as an example case. Popular drive cycles for modern traction motors are scaled down to match the PMSM specifications for laboratory testing. Efficiency determination of the drive cycle is carried out using analytic, numerical, and experimental approaches, enabling the extension of the findings to the real-world EV applications.**

***Index Terms*—drive cycles, electric vehicles, performance maps, permanent magnet synchronous motors, traction motors.**

I. Introduction

The dominance of Permanent Magnet Synchronous Motors (PMSMs) in traction applications is evident, thanks to their exceptional characteristics including high torque and power density, full torque control capabilities even at zero speed, and fast acceleration and deceleration [1]. The PMSM market is likely to grow to $48.6 billion in 2027 at a Compound Annual Growth Rate (CAGR) of 15.4% [2]. With this increasing popularity, there is also a necessity to evaluate the overall performance of these machines for different applications like Electric Vehicles (EVs). Modern electric machines operate across a broad range of torque-speed operating points, necessitating a trade-off between material usage, cost, and energy conversion efficiency [3]. Machine design has long focused on optimizing performance for specific requirements, including acceleration and energy consumption [4]. In the past few years, there has been a growing trend towards the optimization of motor design based on driving cycles, which involves taking into account the efficiency of the machine throughout the entire driving cycle [5], [6]. Clearly, PMSMs outperform Induction Motors (IMs) in terms of torque density and efficiency. Nevertheless, PMSMs do experience drawbacks such as eddy current losses within the magnets at higher speeds. Additionally, when it comes to achieving higher speeds, IMs have an advantage as they can easily engage in field weakening. In contrast, PMSMs require the introduction of supplementary field weakening current, which leads to additional losses. It is important to note that IMs are also subject to rotor cage losses, which affect their performance at both low and high speeds [7]. Simulating a torque-speed profile for a specific drive cycle involves employing electromagnetic models and/or a combination of electromagnetic and thermal models. These simulations are usually performed using time-stepping techniques. However, the accuracy of drive performance and energy conversion efficiency heavily relies on the chosen model, and utilizing such models is time-consuming and computationally intensive [8]. With this, there is always a limitation on evaluation of performance and energy efficiency.

Alternatively, efficiency maps are used to evaluate the performance, which are constructed based on steady-state examinations and do not include transient effects. Experimental validation is typically only performed for a few selected points, so, it is important to have a high degree of accuracy in all operating points [9]. This requires careful experimental validation of these points, which can be tedious. Several ways of investigating the performance of PMSMs have been presented in [9]–[14]. Nevertheless, these investigations are conducted using a specific methodology

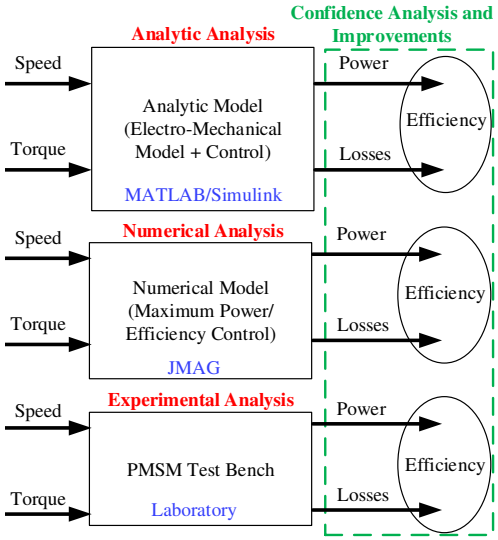

Fig. 1. Workflow of the performance map based analysis.

or through experimental means, and they do not assess the accuracy when compared to alternative approaches for the given scenario. The confidence in using performance maps to analyze dynamic scenarios is often questioned. Efficiencies at different operating points can be determined through analytic, numerical, or experimental methods. By plotting the operating points within a drive cycle on a drive operating area and utilizing performance maps as look-up tables, the drive performance at each operating point can be computed.

This study aims to provide a foundation for addressing fundamental questions regarding the reliability and confidence in using time-stepping solutions compared to performance maps. Furthermore, it seeks to extend the findings into real-world electric vehicle (EV) applications, allowing for practical implementation and application. For the same, some example case real drive cycles are taken as example with reference to a medium range and a small range electric vehicles and they are down-scaled to the ratings of the PMSM available in the lab so as to be able to test in the laboratory. A baseline is established for analytic, numerical, and experimental analysis as shown in Fig. 1. The analytic and numerical methods are introduced, and their respective results are compared.

TABLE I
VEHICLE MOTOR AND LABORATORY MOTOR SPECIFICATIONS [19], [20]

Vehicle Motor Specifications		
Parameters	**Values**	
	BMW i3	**Smart EQ**
Machine Type	PMSM	PMSM
Maximum Torque	250 Nm	160 Nm
Maximum Power	125 kW	60 kW
Base Speed	4800 rpm	3581 rpm
Maximum Speed	11400 rpm	11475 rpm
Lab Motor Specifications		
Parameters	**Values**	
Max. Power	70 W	
Max. Torque	0.15 Nm	
Maximum Speed	7000 rpm	
Inertia	0.000113 kgm^2	
Phase Resistance	8.945 Ω	

II. State of Art of Baseline Determination

Commencing the analysis, the selected approach involves utilizing speed-versus-time drive cycle tests derived from the traction application domain, notably exemplified by the World Harmonized Light Vehicle Test Procedure designed for class 3 vehicles, denoted as WLTP-3. To extract the torque-speed operating points of traction motors with this drive cycle, two test case electric vehicles: a medium range (BMW i3) and a small range (Smart EQ) passenger car are considered. These two electric vehicles are distinct in terms of their performance, range, top speed, efficiency, traction control system, maximum torque, and power. A simple quasi-static longitudinal vehicle model as presented in [15] and also mentioned in [16] is used to compute the torque-speed operating points of the motors used in these vehicles. This enables different torque-speed operating points analyses with different electric motors. For the analysis, an example case of a laboratory scale PMSM is considered.

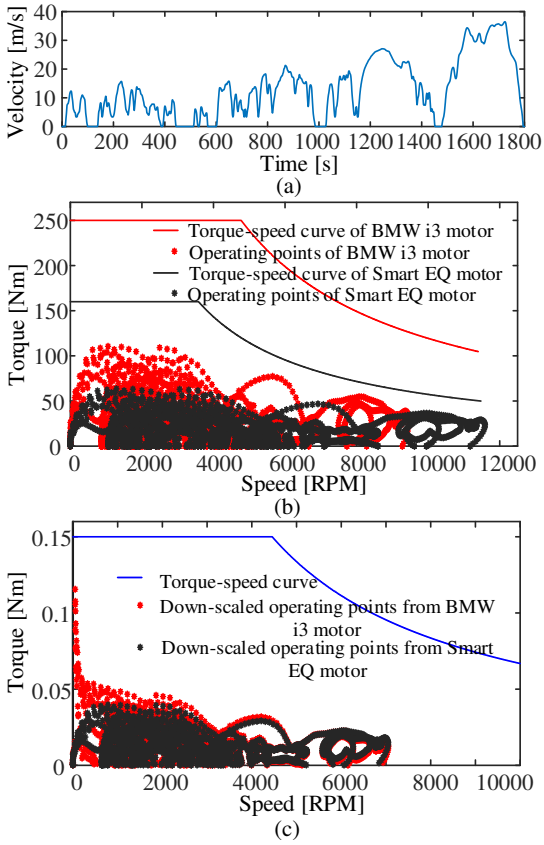

Fig. 2. (a) WLTP class 3 drive cycle, (b) torque-speed operating points of BMW i3 motor and Smart EQ motor on WLTP class 3, (c) down-scaled torque-speed operating points with WLTP class 3 for use with PMSM in the laboratory.

The PMSM test bench has already been available in the laboratory for experimental analysis. The ratings and the

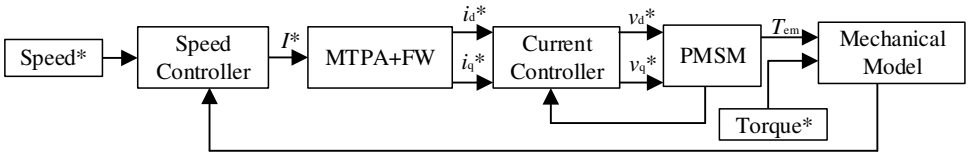

Fig. 3. A cascaded control block diagram of a PMSM; * denotes that the value is commanded.

ranges of the motors used in the example case vehicles are much bigger than those of the PMSM in the laboratory as specified in Table I. Therefore, in order to ensure the compatibility with the test case motor's limitations, the torque-speed operating points are scaled down. This is achieved through the utilization of a mathematical approach that incorporates the motor's parameters as mentioned in [17] and by utilization of a method of down-scaling the drive cycles as presented in [18]. By implementing a down-scaling process, operating points within the feasible range of the laboratory motor are obtained. The torque-speed operating points of the example case vehicle motors and the scaled-down torque-speed operating points for the laboratory based PMSM are shown in Fig. 2.

A. Analytic Model

To investigate the drive cycle performance analytically, the PMSM is modelled in MATLAB/Simulink® environment with all torque-speed operating points as inputs using a time-stepping approach. A cascaded control technique as shown in Fig. 3 is employed, comprising an outer control loop for speed regulation and an inner control loop for current management. The model is simulated in the stationary dq reference frame. Maximum Torque Per Ampere (MTPA) and Field Weakening (FW) techniques are used to generate the corresponding current references. For individual operating points, copper and iron losses are calculated as per (1) and (2) [21].

$$P_{\mathrm{cu}} = (I_{\mathrm{a}}^2 + I_{\mathrm{b}}^2 + I_{\mathrm{c}}^2)R_{\mathrm{phase}} \quad (1)$$

$$P_{\mathrm{core}} = k_{\mathrm{h}} f B_{\mathrm{m}}^2 + k_{\mathrm{e}} f^2 B_{\mathrm{m}}^2 + k_{\mathrm{ex}} f^{1.5} B_{\mathrm{m}}^{1.5} \quad (2)$$

The copper loss in the winding is calculated with Root Mean Square (RMS) phase currents and phase resistance (R_{phase}). The total iron loss in the rotor and the stator core consists of three losses: hysteresis loss, eddy current loss, and excess loss. These losses depend on the peak flux density (B_{m}) and the operating frequency (f). The hysteresis, eddy current, and excess loss coefficients, k_{h}, k_{e}, and k_{ex} respectively, are calculated using curve fitting technique from the manufacturer's data of the steel material used in the motor. For each operating point, with known losses, the percentage efficiency can be calculated using (3). Analyses are also conducted at varying winding temperatures. To keep the analysis straightforward, only the operating points in the first quadrant (motoring mode) of the motor torque-speed profile are considered. The same approach can be applied to the other quadrants as well.

$$\eta = \frac{P_{\mathrm{out}}}{P_{\mathrm{out}} + P_{\mathrm{losses}}} \times 100\% \quad (3)$$

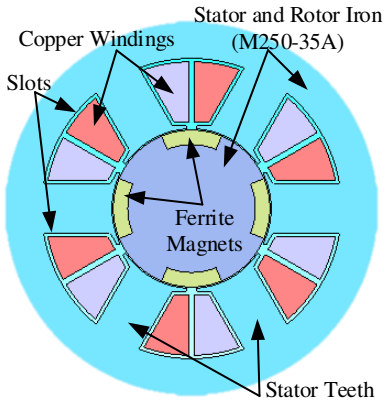

Fig. 4. A 2D FEA model of PMSM visualised in JMAG® [23].

B. Numerical Model

Numerical analysis of the PMSM is conducted utilizing the Finite Element Method (FEM) software JMAG®. The motor model is created with reference to it's geometry specifications and the corresponding materials are assigned as shown in Fig. 4. In the JMAG® environment, a motor response table can be created for each torque-speed operating point. This can basically be considered as a grid and the accuracy on the machine's response depends on the fineness of this grid. Apart from this, element size also known as mesh size plays a vital role in determining the machine's performance accuracy. A fine mesh gives better accuracy but at a cost of larger computational time and vice-versa. The relationship between mesh size and the computational time is not linear but rather depends on various factors, including the specific nature of the simulation problem, the FEM software, and the hardware capabilities. A general rule of thumb is that reducing the mesh size by half increases the number of elements (and nodes) by a factor of four (assuming a regular grid), leading to a significant increase in computational workload. So, in numerical context, the overall performance of the computation is a trade-off between the accuracy and the computational time. Like in the analytic method, only copper and iron losses are considered for the efficiency map calculation. Analyses are also made for different winding temperatures. A preset 1 method is used where hysteresis losses are determined using a hysteresis loop and joule losses are determined with Fast Fourier Transform (FFT) method as described in [22].

III. Results and Discussions

For the drive cycle, the different torque-speed operating points of the PMSM are obtained with respect to two different electric vehicles. This resulted in a total of two different sets

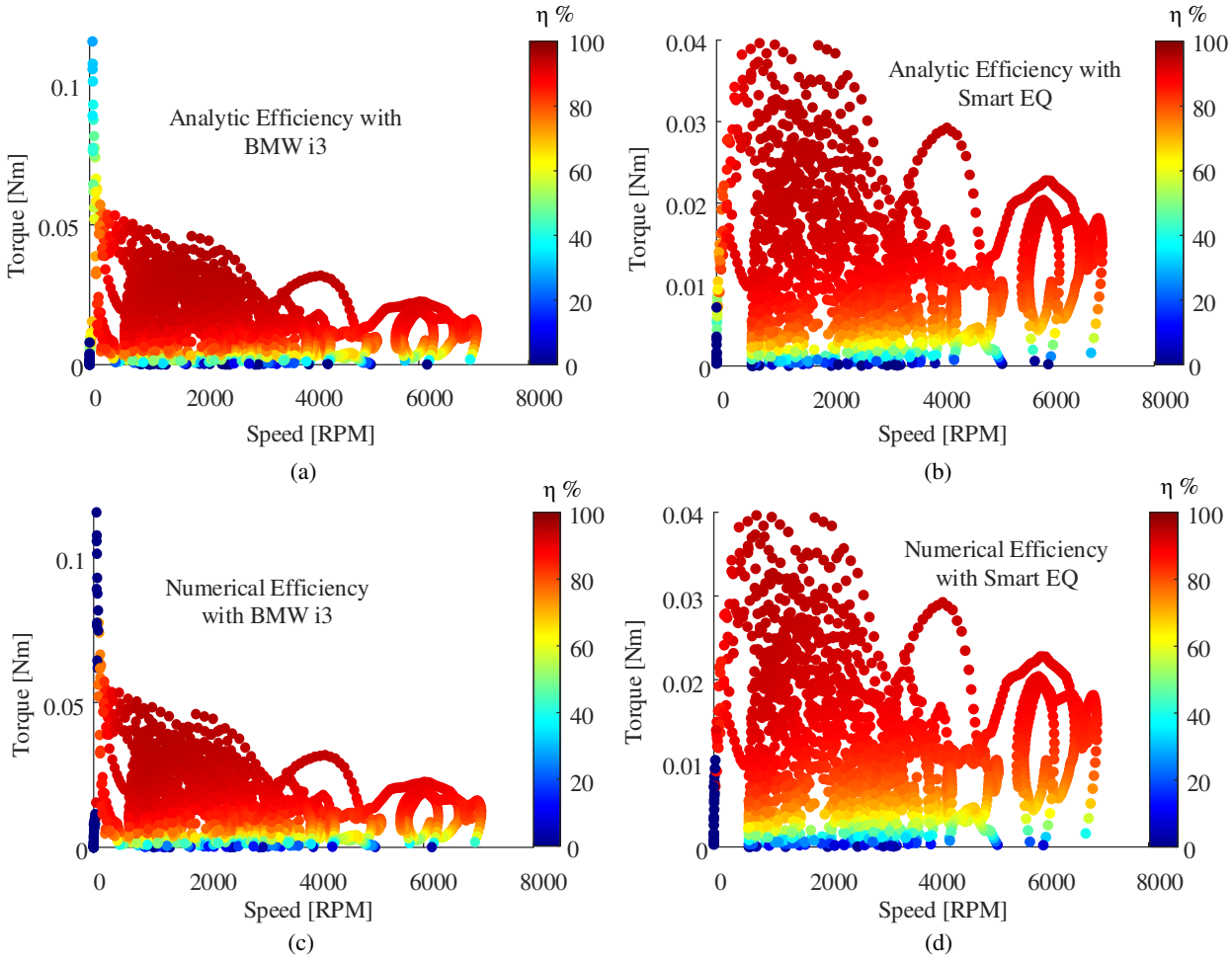

Fig. 5. Efficiency plots of PMSM: (a) analytic result with operating points obtained from BMW i3 motor, (b) analytic result with operating points obtained from Smart EQ motor, (c) numerical result with operating points obtained from BMW i3 motor, (d) numerical result with operating points obtained from Smart EQ motor.

of torque-speed operating points for the analysis. Both analytic and numerical studies have been conducted and comparisons in terms of energy conversion efficiency over a drive cycle were made. Fig. 5 presents the efficiency plots of the PMSM operating points with respect to two different vehicles, derived through both analytic and numerical analyses and plotted using a scatter plot method.

As per visual comparison, the results obtained through both methods appear to exhibit similarities and, in some instances, exact agreement. This observation underscores the effectiveness of the described baseline analysis method. The comparisons were specifically conducted in three key regions: (a) high-speed, low-torque region, (b) low-speed, high-torque region, and (c) region where both speed and torque are relatively high. In all instances, it is evident that regions with lower torque exhibit lower efficiency. Both the high-torque, low-speed, and low-torque, high-speed regions are relatively less efficient when compared to the operational region where both torque and speed fall within medium ranges. The notable variation is primarily observed within the high-speed range, as well as in situations characterized by low load and medium speeds.

To better compare the efficiencies at different operating points resulting from both the analytic and the numerical method, the efficiencies are plotted against time as shown in Fig. 6. As it can be easily noted that the results with the two different methods are quite similar with relatively smaller error in some operating areas. Although these errors are small, they are not negligible. These variations arise due to uncertainties in the motor parameters, inverter control methods, and settings of the Finite Element Analysis (FEA), such as mesh size.

To explore the similarity, the Root Mean Square Error (RMSE) is utilized to compare the analytically derived drive cycle efficiency with the numerically calculated values as indicated in (4). In this context, n denotes the number of operating points, m_{i} denotes the efficiency calculated analytically, and s_{i} denotes the efficiency calculated numerically, for each operating point respectively.

$$E = \sqrt{\frac{1}{n}\sum_{i=1}^{n} |m_{\mathrm{i}} - s_{\mathrm{i}}|^2} \tag{4}$$

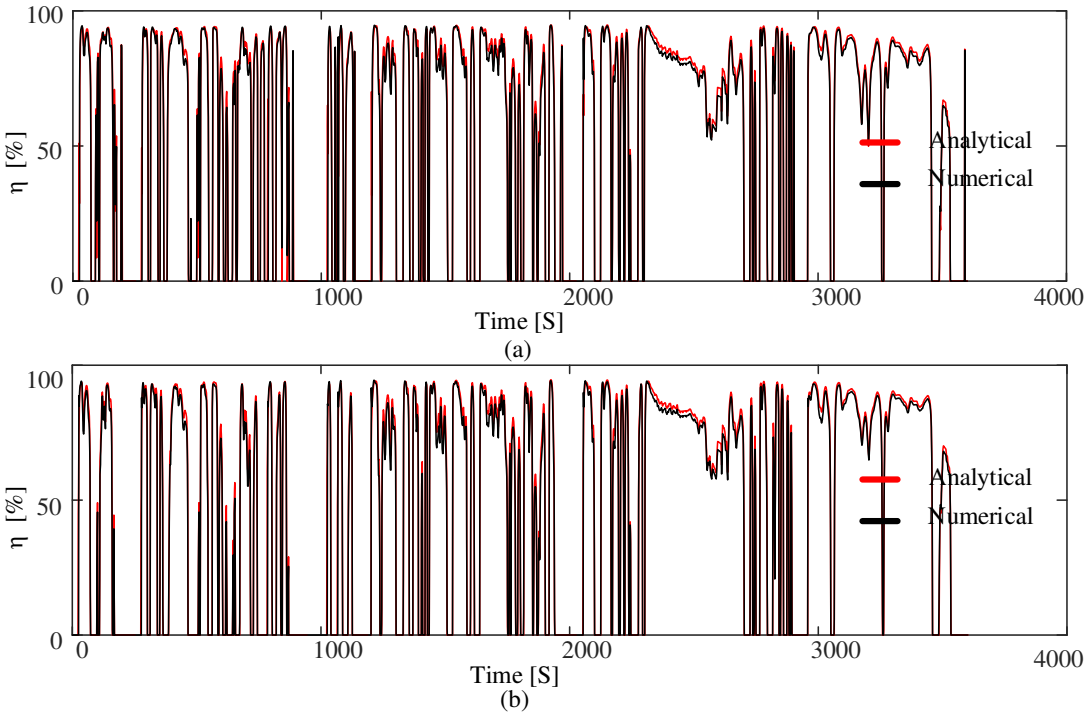

Fig. 6. Computed efficiencies for the different operating points of the PMSM obtained from: (a) BMW i3 motor, (b) Smart EQ motor, both for the WLTP class 3 drive cycle.

The RMSE between the analytic and the numerical efficiency values for the PMSM operating points obtained with respect to the mid-range vehicle (BMW i3) is 4.91 and for operating points with small-range (Smart EQ), it is 4.09. It signals that the similarity might differ when using operating points deduced from different vehicle types and in this case, with the Smart EQ, this error is smaller.

Furthermore, to examine the impact of changes in winding temperature, the operating points are simulated both analytically and numerically at different stator winding temperatures. While the results presented are for 25°C (room temperature), additional sets of results for 40°C and 100°C are also analyzed. The RMSE values of analytically and numerically simulated efficiency results of the operating points for different winding temperature with respect to two different vehicles are shown in Fig. 7. The deviations are comparatively larger for the BMW i3 than for the Smart EQ. There are minor variations between the analytical and the numerical results. These are primarily explained by the model inaccuracies. So, in this case, use of a correct winding temperature is much less important than the suitable choice of the model.

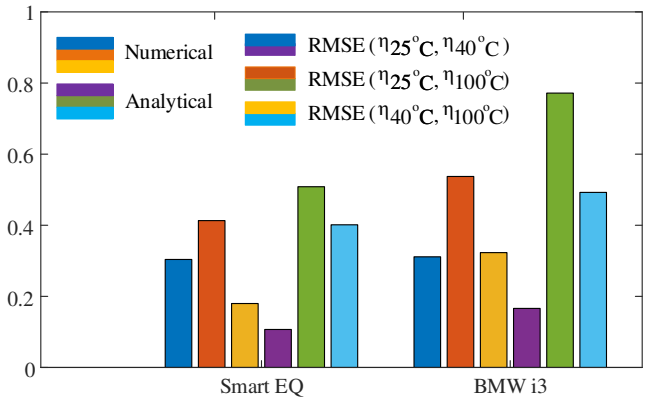

Fig. 7. Root mean square error of efficiency values of operating points of PMSM for different winding temperatures.

IV. Conclusions

This study compares the confidence of using different time-stepping solutions for PMSMs in various drive cycle operating scenarios. An example case drive cycle is examined, involving two different electric vehicles and the corresponding torque-speed operating points of a small PMSM available in the laboratory. Analytic and numerical methods are employed to analyze the PMSM's performance at all operating points, with close comparisons between the two approaches revealing that the suitable choice of the type of model is much more important than the use of the correct temperature. The motor showcases efficient performance in the medium speed and medium torque regions, although noticeable differences between the methods arise in high-speed and high-load regions.

This analysis provides valuable insights into the accuracy and reliability of the analytic and numerical approach in describing the motor's efficiency under various operating conditions. Further investigation will entail experimental testing of the PMSM in the laboratory, encompassing all torque-speed operating points considered in the baseline assessment with various drive cycles.

ACKNOWLEDGMENT

This work is supported by the joint DFG/FWF Collaborative Research Centre CREATOR (CRC – TRR361/F90) at TU Darmstadt, TU Graz, and JKU Linz.

REFERENCES

[1] E. Agamloh, A. von Jouanne, and A. Yokochi, 'An Overview of Electric Machine Trends in Modern Electric Vehicles', Machines, vol. 8, no. 2, p. 20, Apr. 2020, doi: 10.3390/machines8020020.

[2] The Business Research Company, 'Permanent Magnet Synchronous Motor (PMSM) Global Market Report 2023'. https://www.researchandmarkets.com/reports/5741705/permanent-magnet-synchronous-motor-pmsm-global (accessed Jun. 09, 2023).

[3] Husain et al., 'Electric Drive Technology Trends, Challenges, and Opportunities for Future Electric Vehicles', Proceedings of the IEEE, vol. 109, no. 6, pp. 1039–1059, Jun. 2021, doi: 10.1109/JPROC.2020.3046112.

[4] E. A. Grunditz, T. Thiringer, and N. Saadat, 'Acceleration, Drive Cycle Efficiency, and Cost Tradeoffs for Scaled Electric Vehicle Drive System', IEEE Trans. on Ind. Applicat., vol. 56, no. 3, pp. 3020–3033, May 2020, doi: 10.1109/TIA.2020.2976861.

[5] S. Pastellides, S. Gerber, R.-J. Wang, and M. Kamper, 'Evaluation of Drive Cycle-Based Traction Motor Design Strategies Using Gradient Optimisation', Energies, vol. 15, no. 3, p. 1095, Feb. 2022, doi: 10.3390/en15031095.

[6] L. Dang, N. Bernard, N. Bracikowski, and G. Berthiau, 'Design Optimization with Flux Weakening of High-Speed PMSM for Electrical Vehicle Considering the Driving Cycle', IEEE Trans. Ind. Electron., vol. 64, no. 12, pp. 9834–9843, Dec. 2017, doi: 10.1109/TIE.2017.2726962.

[7] G. Pellegrino, A. Vagati, B. Boazzo, and P. Guglielmi, 'Comparison of Induction and PM Synchronous Motor Drives for EV Application Including Design Examples', IEEE Trans. on Ind. Applicat., vol. 48, no. 6, pp. 2322–2332, Nov. 2012, doi: 10.1109/TIA.2012.2227092.

[8] M. Salameh, I. P. Brown, and M. Krishnamurthy, 'Driving Cycle Analysis Methods Using Data Clustering for Machine Design Optimization', in 2019 IEEE Transportation Electrification Conference and Expo (ITEC), Detroit, MI, USA: IEEE, Jun. 2019, pp. 1–6. doi: 10.1109/ITEC.2019.8790523.

[9] A. Mahmoudi, W. L. Soong, G. Pellegrino, and E. Armando, 'Efficiency maps of electrical machines', in 2015 IEEE Energy Conversion Congress and Exposition (ECCE), Sep. 2015, pp. 2791–2799. doi: 10.1109/ECCE.2015.7310051.

[10] H. Sano, K. Semba, Y. Suzuki, and T. Yamada, 'Investigation in the accuracy of FEA Based Efficiency Maps for PMSM traction machines', in 2022 International Conference on Electrical Machines (ICEM), Sep. 2022, pp. 2061–2066. doi: 10.1109/ICEM51905.2022.9910824.

[11] S. Ferrari, P. Ragazzo, G. Dilevrano, and G. Pellegrino, 'Flux-Map Based FEA Evaluation of Synchronous Machine Efficiency Maps', in 2021 IEEE Workshop on Electrical Machines Design, Control and Diagnosis (WEMDCD), Apr. 2021, pp. 76–81. doi: 10.1109/WEMDCD51469.2021.9425678.

[12] R. Bojoi, E. Armando, M. Pastorelli, and K. Lang, 'Efficiency and loss mapping of AC motors using advanced testing tools', in 2016 XXII International Conference on Electrical Machines (ICEM), Sep. 2016, pp. 1043–1049. doi: 10.1109/ICELMACH.2016.7732654.

[13] E. Roshandel, A. Mahmoudi, S. Kahourzade, A. Yazdani, and G. M. Shafiullah, 'Losses in Efficiency Maps of Electric Vehicles: An Overview', Energies, vol. 14, no. 22, Art. no. 22, Jan. 2021, doi: 10.3390/en14227805.

[14] T. A. Huynh and M.-F. Hsieh, 'Performance Analysis of Permanent Magnet Motors for Electric Vehicles (EV) Traction Considering Driving Cycles', Energies, vol. 11, no. 6, Art. no. 6, Jun. 2018, doi: 10.3390/en11061385.

[15] L. Guzzella and A. Amstutz, 'The QSS Toolbox Manual'. Jun. 2005. [Online]. Available: https://idsc.ethz.ch/research-guzzella-onder/downloads.html

[16] G. Gagliardi, A. Casavola, W. Nesci, and G. Prodi, 'A quasi-static simulation tool for the design and optimization of hybrid powertrains', Sep. 2012.

[17] M. D. Petersheim and S. N. Brennan, 'Scaling of hybrid electric vehicle powertrain components for hardware-in-the-loop simulation', in 2008 IEEE International Conference on Control Applications, Sep. 2008, pp. 720–726. doi: 10.1109/CCA.2008.4629602.

[18] P.K. Dhakal, K. Heidarikani, and A. Muetze, 'Down-scaling of drive cycles for experimental drive cycle analyses', in 12th International Conference on Power Electronics, Machines and Drives (PEMD 2023), Brussels, Belgium, Oct. 2023.

[19] 'Technical Data BMW i3 (120Ah)'. https://www.press.bmwgroup.com/global/article/detail/T0148284EN/the-bmw-i3?language=en (accessed Jan. 09, 2023).

[20] 'Smart EQ fortwo coupe', EV Database. https://ev-database.org/car/1230/Smart-EQ-fortwo-coupe (accessed Jan. 09, 2023).

[21] P. T. Luu, J.-Y. Lee, J.-H. Lee, and J.-W. Park, 'Electromagnetic and Thermal Analysis of Permanent-Magnet Synchronous Motors for Cooperative Robot Applications', IEEE Transactions on Magnetics, vol. 56, no. 3, pp. 1–4, Mar. 2020, doi: 10.1109/TMAG.2019.2942939.

[22] '[JFT173] Workflow and Key Points in Efficiency Map Analysis — Simulation Technology for Electromechanical Design : JMAG'. https://www.jmag-international.com/tutorial/jft173_efficiencymapbasic/download/ (accessed Jun. 12, 2023).

[23] 'Simulation Technology for Electromechanical Design: JMAG'. [Online]. Available: https://www.jmag-international.com/